

Intraplate and interplate faulting interactions during the August 31, 2012, Philippine Trench earthquake (M_w 7.6) sequence

Lingling Ye,¹ Thorne Lay,¹ and Hiroo Kanamori²

Received 11 October 2012; revised 9 November 2012; accepted 12 November 2012; published 28 December 2012.

[1] On August 31, 2012, a large (M_w 7.6) thrust earthquake occurred within the subducting Philippine Sea plate seaward of a low seismicity region of the plate boundary (9.5°N–11.5°N), possibly as a result of horizontal compressional stress accumulation offshore of a locked megathrust. The mainshock ruptured from ~30–50 km depth, with high radiated-energy/seismic-moment ratio and enriched short-period P-wave radiation. The nine largest aftershocks with global centroid moment tensor solutions (M_w ~5.2–5.6) were shallow (10–13 km) normal-faulting outer-rise events, and a waveform template analysis using regional broadband data indicates many (48/110) similar normal faulting events (m_b 4.0–5.5) and a few (8/110) likely shallow thrust faulting events on the megathrust with additional very small unidentified events. Coulomb stress perturbations may contribute to the mix of intraplate and interplate faulting. Geodetic assessment of any slip deficit on the megathrust is essential for quantifying the potential for a future large interplate rupture in this region. **Citation:** Ye, L., T. Lay, and H. Kanamori (2012), Intraplate and interplate faulting interactions during the August 31, 2012, Philippine Trench earthquake (M_w 7.6) sequence, *Geophys. Res. Lett.*, 39, L24310, doi:10.1029/2012GL054164.

1. Introduction

[2] Large thrust-faulting earthquakes within subducting plates seaward of plate boundaries are rare, but have been observed to correlate with subsequent occurrence of great thrust events on the adjacent megathrusts [Christensen and Ruff, 1988]. Together with the common occurrence of normal faulting seaward of the plate boundary following large megathrust events and temporal patterns of deeper slab activity, it has been proposed that intraplate elastic stresses offshore and down-dip of the megathrust are modulated by the fluctuating cycle of locking and rupturing of the plate boundary [Dmowska et al., 1988; Lay et al., 1989, 2009, 2011; Taylor et al., 1996; Ammon et al., 2008]. Thus, occurrence of a large outer rise or outer trench slope thrust earthquake is of interest as a possible indicator of interplate coupling and strain accumulation prior to a future interplate

rupture. We examine the earthquake sequence associated with a large thrust earthquake below the Philippine Trench seaward of a plate boundary megathrust region with uncertain seismic potential.

2. The 2012 M_w 7.6 Philippine Trench Earthquake

[3] The Philippines region has extensive large earthquake activity documented back to 1600 [e.g., Bautista and Oike, 2000; Abe, 1994; Allen et al., 2009] (Figure 1) involving several subduction zones and the long Philippine Fault. On August 31, 2012, an M_w 7.6 earthquake struck beneath the Philippine Trench (10.838°N, 126.704°E, hypocentral depth 34.9 km, 12:47:34 UTC (USGS NEIC, <http://earthquake.usgs.gov/earthquakes/>)). Long-period seismic waves used in a W-phase inversion indicate a centroid depth of 44 to 50 km (Figure 2b), which is comparable to depths for other well-studied large thrust events near oceanic trenches [Christensen and Ruff, 1988; Lay et al., 2009; Raeesi and Atakan, 2009; Todd and Lay, 2012]. Elastic bending stresses in subducting plates might account for relatively deep thrust activity below shallower normal faulting activity [e.g., Chapple and Forsyth, 1979; Lay et al., 1989], but very large trench slope thrust events may require that interplate locking decrease the depth of the elastic bending neutral surface in the plate, bringing a larger fraction of the brittle lithosphere into the compressional regime [e.g., Taylor et al., 1996; Liu and McNally, 1993].

[4] The 2012 Philippine Trench event is located offshore of a region of the subduction zone from 9.5°N–11.5°N, where there is no record of great earthquake activity dating back to 1600 (Figure 1), and there is large uncertainty in the seismic potential [Bautista and Oike, 2000; Nishenko, 1991]. This region also has had few moderate size events with $m_b \geq 5.0$ since 1973 (see Figure S1 in the auxiliary material), so it can be described as a low seismicity region extending 150–200 km along the trench.¹ The adjacent portions of the subduction zone have experienced large earthquakes (Figure 1): the October 18, 1897 northern Samar (M_s 7.3) earthquake struck to the north and the April 14, 1924 (M_s 8.2) event struck eastern Mindanao to the south. The faulting geometries of these events are not known. There have been large intraplate normal-faulting events to the north and south, for example the October 31, 1975 (M_w 7.6) event involved normal faulting [Christensen and Ruff, 1988]. There is no clear disruption of the trench bathymetry, upper

¹Department of Earth and Planetary Sciences, University of California, Santa Cruz, California, USA.

²Seismological Laboratory, California Institute of Technology, Pasadena, California, USA.

Corresponding author: T. Lay, Department of Earth and Planetary Sciences, University of California, 1156 High St., Santa Cruz, CA 95064, USA. (tlay@ucsc.edu)

¹Auxiliary materials are available in the HTML. doi:10.1029/2012GL054164.

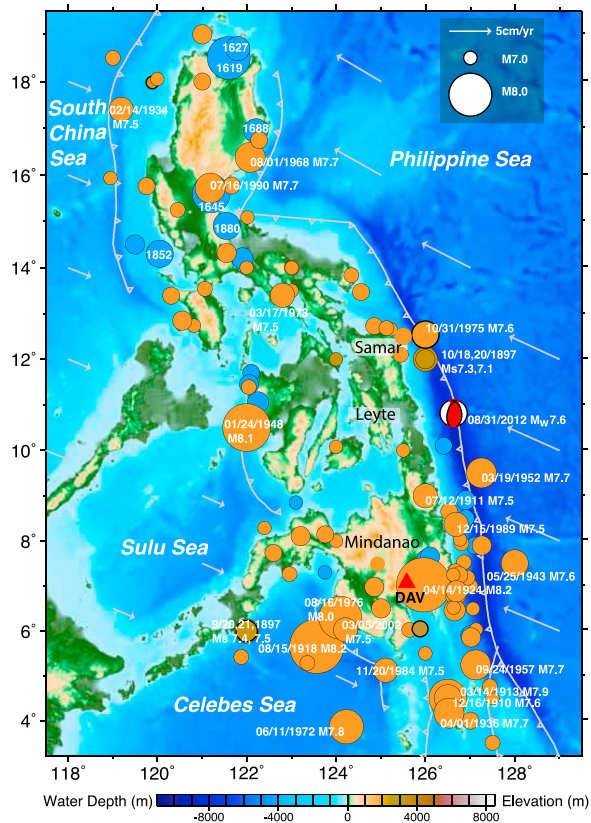


Figure 1. Large earthquakes around the Philippines: blue circles are $M \sim 7+$ events (inferred from Intensity information) from 1600 to 1895 [Bautista and Oike, 2000], the brown circles are large events in 1897 with M_s from Abe [1994], including the northern Samar event of October 18, 1897 (M_s 7.3), and orange circles are $M \geq 7.0$ events from 1900 to 2008 from PAGER-CAT [Allen et al., 2009]. The red focal mechanism is the W-Phase solution for the August 31, 2012 Philippine Trench event plotted at the NEIC epicenter. The red triangle shows the location of GSN station DAV. Barbed curves indicate subduction zones. Arrows indicate plate motion directions and rates computed using model GSRM 1.2 [Kremer et al., 2003].

plate structure or incoming bathymetric features on the Philippine Sea plate that might suggest distinct coupling of the megathrust in this region [Bilek et al., 2003; Song and Simons, 2003]. Relatively sparse observations of GPS velocities indicate east-west compressional strain across the southern Philippines [e.g., Rangin et al., 1999] and convergence in the Philippine Trench varies from 5.4 cm/yr near 13°N to 3.2 cm/yr near 7°N [Yumul et al., 2008]. However, the relative contributions of internal upper plate deformation, especially near the Philippine fault, and any plate boundary localized slip deficit in the central Philippine trench are not well-established by published GPS observations.

[5] The point-source moment tensor for the August 31, 2012 event was determined by W-phase inversion using three-component observations from 64 channels at 47 Global Seismic Network (GSN) stations for the passband 0.00167–0.005 Hz. The scalar moment is 3.2×10^{20} N-m, with the optimal centroid depth of 50.5 km yielding the solution shown in Figure 2. Corresponding waveform fits are shown in Figure S2. The depth appears to be quite well constrained and the centroid location is 11°N , 127°E . The solution has a minor non-double-couple component.

[6] Using the two possible fault plane geometries from the best double-couple for the W-phase moment tensor (Figure 2), we performed finite-fault inversions using 81 teleseismic broadband P waves with 75 s long signals. Comparable fits were obtained using either nodal plane, and we show the result for a fault model with strike $\phi = 348.2^\circ$ and dip $\delta = 40.1^\circ$ in Figure 3a. We assumed the hypocentral depth of 35 km from the NEIC location, but found little resolution of hypocenter between 30 km and 45 km depth. A rupture velocity of 3 km/s was assumed, and the subfaults were parameterized to have 4 overlapping 2-s duration triangles (allowing total subfault duration of up to 5 s), with variable rake. A large slip concentration is found near the hypocenter, with rupture extending from 25–55 km in depth and about 50 km along strike, with greater extent toward the SSE. The moment rate function (Figure 3b) has jagged short-duration pulses over a 25-s duration, stemming from short period roughness in the P waves (waveforms and fits are shown in Figure S3). If we evaluate the stress drop over the well-resolved part of the fault model with subfault moments at least 12% of the peak

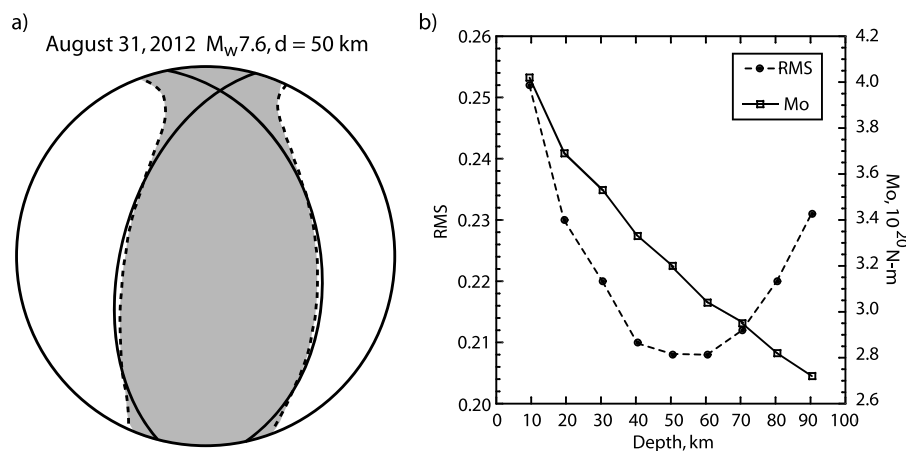


Figure 2. (a) Point-source moment tensor from W-phase inversion for the August 31, 2012 Philippine event. The best double couple for a source depth of 50 km has nodal plane orientations: strike, $\phi_1 = 348.2^\circ$, dip, $\delta_1 = 40.1^\circ$, rake, $\lambda_1 = 68.9^\circ$; and $\phi_2 = 195^\circ$, $\delta_2 = 53.0^\circ$, $\lambda_2 = 106.9^\circ$. The waveform fits are shown in Figure S2. (b) W-phase inversion RMS and estimated seismic moment, M_o , dependence on assumed source depth. A centroid time of 15 s was used.

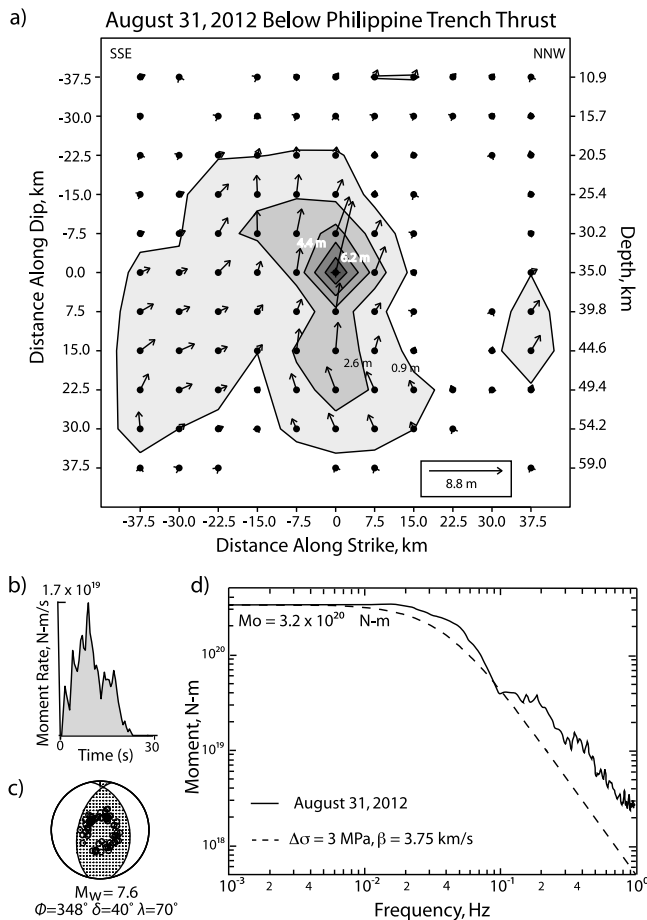


Figure 3. (a) Rupture model slip distribution for the August 31, 2012 Philippine event obtained by inverting 81 75-s long teleseismic P wave signals for a fault plane with $\phi = 348.2^\circ$ and $\delta = 40.1^\circ$. The vectors indicate the direction of slip of the hanging-wall side of the fault relative to the foot-wall. (b) The ~ 25 s duration moment rate function for the slip model, with a centroid time of 10 s. (c) Average focal mechanism with P wave sampling of the focal sphere. Waveform fits are shown in Figure S3. (d) The average far-field P wave source spectrum is shown by the black line, estimated at frequencies less than ~ 0.03 Hz from the moment rate function in Figure 3b and at frequencies $> \sim 0.03$ Hz from stacking of broadband teleseismic P wave spectra. The dashed line is a reference source spectrum for an ω^{-2} model with 3 MPa stress drop, shear velocity, $\beta = 3.75$ km/s, and seismic moment given by the W-phase inversion in Figure 2.

subfault moment, the estimated slip area is 2300 km^2 , the moment is $3.2 \times 10^{20} \text{ N-m}$, the static stress drop is $\sim 7 \text{ MPa}$ (assuming a circular rupture), and the average slip is $\sim 2.0 \text{ m}$. Similar results are found using the conjugate plane (Figure S4).

[7] The enriched level of short-period energy in the P waveforms is particularly evident in the average source spectrum shown in Figure 3d compared to a reference ω^{-2} spectrum with 3 MPa stress parameter. The spectrum is obtained from the moment rate function for frequencies below ~ 0.03 Hz and from stacking of 41 broadband P-wave spectra for higher frequencies. The radiated energy is

estimated as $E_r = 1.6 \times 10^{16} \text{ J}$ over the frequency range 0–1.0 Hz (following Venkataraman and Kanamori [2004]). There is some additional energy at higher frequencies that we have not accounted for. The USGS estimate of energy is $1.8 \times 10^{16} \text{ J}$, which is quite compatible. The E_r/M_o ratio we obtain is 5.0×10^{-5} , which is relatively high even among large intraplate ruptures (Figure S5).

3. Aftershock Sequence Characterization

[8] A substantial aftershock sequence (Figure 4a) occurred following the mainshock, with events having M_w up to 5.6. Nine of the larger events (N1–N9 in Figure 4a) have Global Centroid Moment Tensor (GCMT, <http://www.globalcmt.org>) solutions, all of which have shallow (10–13 km centroid depth) normal faulting mechanisms, all but one are clustered near the trench south of the mainshock. A total of 110 distinct aftershocks with $m_b \geq 4.0$ were listed in the NEIC and PHIVOLCS (Philippine Institute of Volcanology and Seismology) bulletins from August 31 to September 16, 2012.

[9] We attempted to identify events with faulting mechanisms similar to the mainshock that might be on the main rupture plane, hoping to resolve between the two nodal planes. We used broadband vertical component recordings of the aftershocks at regional GSN station DAV about 350 km to the south-southwest (Figure 1), filtered in passbands of 0.01–0.03 Hz and 0.01–0.02 Hz to evaluate distinct waveform clusters using template waveforms (Figure S6). One of the normal faulting aftershocks (N1) was found to have good waveform correlations with 56 of the aftershocks (Figure 4), while 8 other events have distinct waveforms similar to those for an event on December 29, 2009, for which a GCMT mechanism indicates shallow-dipping thrust faulting. The other events are all very small at DAV and their mechanisms are uncertain. The aftershock sequence (Figure 4c) thus appears to be dominated by shallow near-trench normal faulting with a patch of triggered thrust-faulting apparently on or near the megathrust to the west. GCMT solutions for prior earthquakes in the region (at NEIC epicenters in Figure 4a) indicate deeper thrust faulting near the southern end of the seismic gap zone. The aftershocks do not reveal which nodal plane ruptured for the main event, but they do indicate activation of distinct fault systems by the mainshock.

4. Faulting Interactions

[10] The aftershock sequence likely involves both intraplate and interplate faulting. While dynamic triggering produced by the strong waves from the mainshock may play an important role in activating different fault systems, static stress changes may as well. There are several recent examples of large shallow normal faulting events being followed by deeper thrust events below the outer trench slope in the Kuril Islands [Lay et al., 2009] and in northern Kermadec [Todd and Lay, 2012]. There has also been clear activation of megathrust faulting by large trench-slope normal faulting in Tonga [Lay et al., 2010] and northern Kermadec [Todd and Lay, 2012]. Seismic activity can also be suppressed by stress changes from large faulting [Toda et al., 2012], although the seismicity in the central Philippines Trench region has been too sparse to detect regional decreases.

[11] We compute Coulomb stress changes induced on the shallow normal faulting and interplate thrust faulting

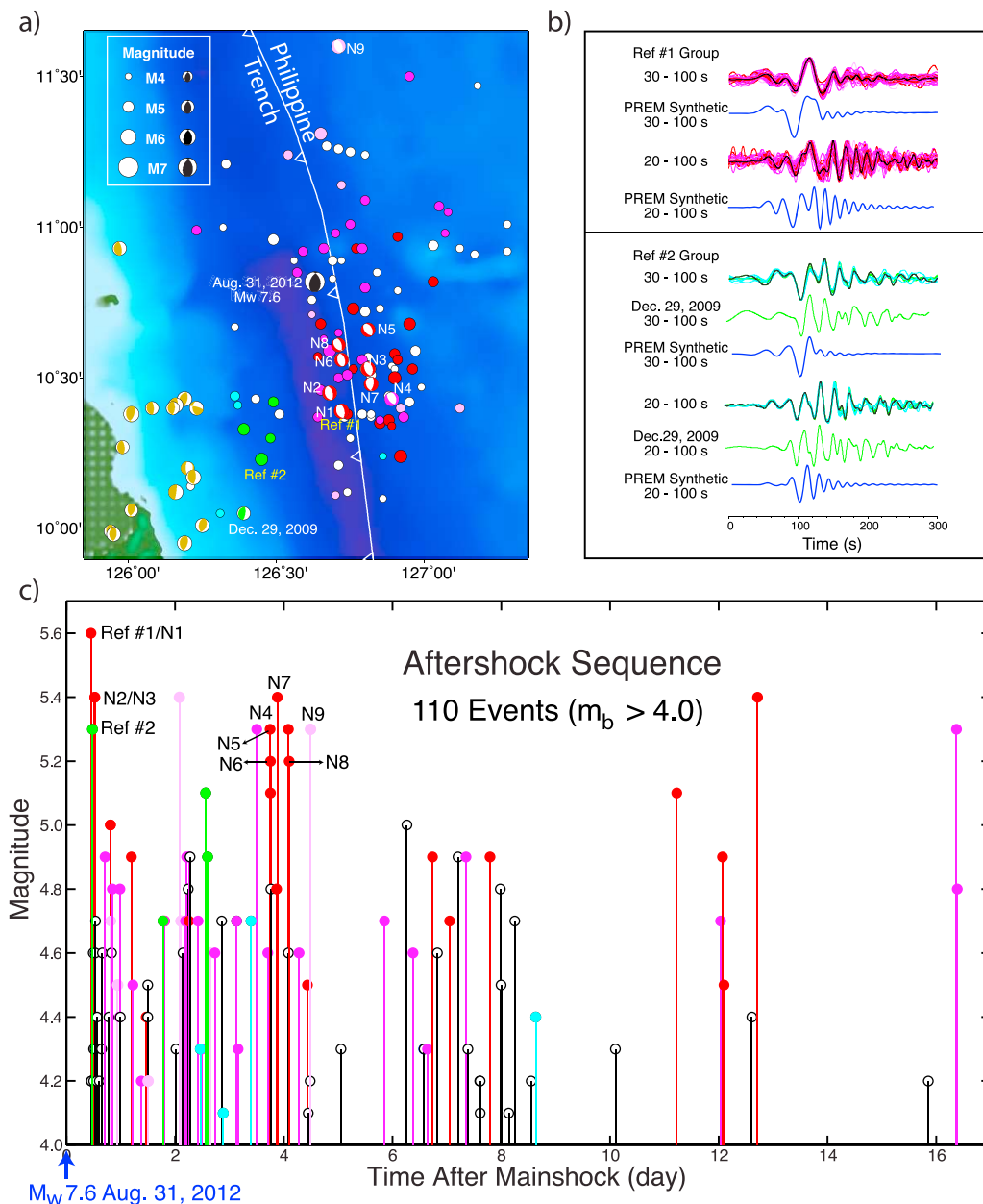


Figure 4. (a) Locations of events in the aftershock sequence from combined catalogs of NEIC and PHIVOLCS (Philippine Institute of Volcanology and Seismology), and GCMT focal mechanisms of earlier events (brown mechanisms and December 29, 2009 underthrusting event). The black mechanism is the GCMT solution for the August 31, 2012 mainshock. The red, pink, and pale pink symbols (including GCMT mechanisms) indicate similarity of waveforms at station DAV to that for normal-faulting reference event #1: with very high waveform cross-correlation coefficients (≥ 0.9 for 30–100 s and ≥ 0.7 for 20–100 s), high cross-correlation coefficients (≥ 0.8 for 30–100 s and ≥ 0.5 for 20–100 s), and medium coefficients (≥ 0.8 for 30–100 s waveform, but < 0.5 for 20–100 s), respectively. The green and cyan symbols indicate events with very high or high cross-correlation coefficients with reference event #2 waveforms, including the December 29, 2009 event. White circles are events with no classification of mechanism. The white barbed curve indicates the position of the trench. (b) Superimposed waveforms for the groups of events similar to the two template waveforms in two pass bands, along with synthetic seismograms for station DAV. For group 2, the very highly correlated December 29, 2009 waveform is shown as well, indicating that these are likely shallow thrust events. (c) Time series for the aftershock sequence color-coded as in the map, indicating the predominance of normal faulting throughout the sequence.

geometries that were activated in the aftershock sequence (Figure 5). Figures 5b and 5c show cross sections through the stress change volume calculated for the mainshock slip model in Figure 3 with target fault geometries corresponding

to the two populations of waveforms found in the aftershocks. Figure 5b indicates that several bar increase in driving stress is likely for normal faulting events above the deep thrust event in the vicinity of the observed cluster of normal

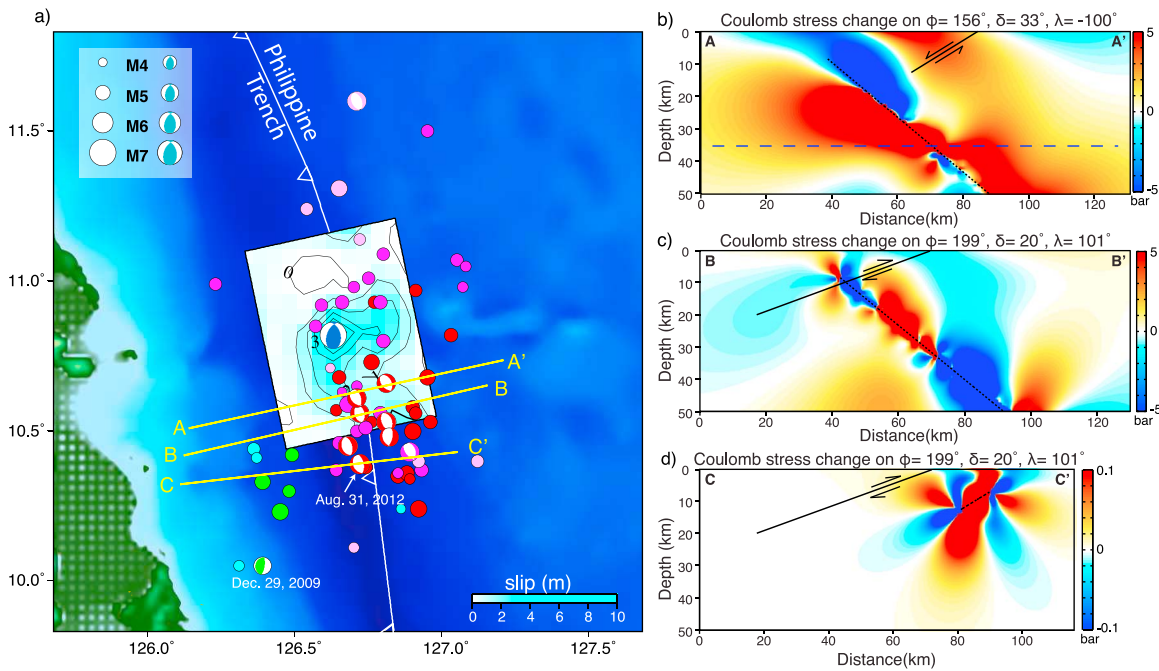


Figure 5. (a) Map view of the slip model (Figure 3) for the August 31, 2012 Philippine event with aftershock locations from NEIC and PHIVOLCS indicated by dots and GCMT focal mechanisms color-coded as in Figure 4. Positions of three cross-section, AA', BB' and CC', are indicated for which the Coulomb stress changes are computed in vertical profiles. (b) Vertical cross section showing Coulomb stress change calculated for the mainshock finite fault model (dotted line) on target normal faults with the GCMT geometry (black solid line) of shallow reference event #1. (c) Coulomb stress change calculated for the mainshock finite fault model (dotted line) on target shallow dipping thrust faults with the GCMT geometry of the December 29, 2009 event (black solid line). (d) Coulomb stress change calculated for a uniform slip model for the M_w 5.5 normal faulting reference event #1 (dotted line) on shallow dipping thrust faults with the GCMT geometry of the December 29, 2009 event (black solid line).

fault aftershocks. Figure 5c indicates that the driving stress on the megathrust produced by the mainshock decreased at depths larger than 10 km, but there may have been about a 1 bar increase in the shallowest part of the megathrust where the observed thrust aftershocks occurred. Comparable stress changes are predicted for a slip model using the alternate mainshock rupture plane, as shown in Figure S7. The normal faulting at shallow depth involves only small events, but a large number of them occurred, and these should have produced small increases in driving stress (fractional bar increases per event) on the shallow megathrust as well. It is difficult to further characterize the faulting interactions, especially since we are ignorant of the precise aftershock faulting geometries and the ambient stress regimes that the stress perturbations are superimposed on, but this is another clear case of complex faulting interactions in the shallow subduction zone.

5. Conclusions

[12] The August 31, 2012, M_w 7.6 earthquake below the Philippine trench is a high energy release thrust-faulting event that ruptured from about 25–55 km deep in the subducting plate offshore of a long-term seismic gap of uncertain seismic potential. The thrust mechanism may indicate strong interplate coupling along the megathrust from 9.5°N–11.5°N, but that possibility requires direct evaluation by geodetic mapping of strain within the upper plate. The long time interval (>400 years) over which there is no documented larger interplate rupture in this region, combined

with the ~ 5 cm/yr convergence rate, suggest the potential for a great earthquake in this region if it is significantly seismically coupled. The shallow normal faulting that dominates the aftershock sequence and the triggering of what appears to be very shallow megathrust events represents interaction between different fault systems in the subduction zone, but does not establish whether interplate strain accumulation is occurring.

[13] **Acknowledgments.** This work made use of GMT and SAC software. Coulomb 3 software produced by S. Toda, R. Stein, J. Lin, and V. Sevilgen was used. The IRIS DMS data center was used to access the seismic data from Global Seismic Network and Federation of Digital Seismic Network stations. We thank two anonymous reviewers for their helpful comments on the manuscript. This work was supported by NSF grants EAR0635570 (T. L.).

[14] The Editor thanks two anonymous reviewers for their assistance in evaluating this paper.

References

- Abe, K. (1994), Instrumental magnitudes of historical earthquakes, 1892 to 1898, *Bull. Seismol. Soc. Am.*, *84*, 415–425.
- Allen, T. I., K. D. Marano, P. S. Earle, and D. J. Wald (2009), PAGER-CAT: A composite earthquake catalog for calibrating global fatality models, *Seismol. Res. Lett.*, *80*, 57–62, doi:10.1785/gssrl.80.1.57.
- Ammon, C. J., H. Kanamori, and T. Lay (2008), A great earthquake doublet and seismic stress transfer cycle in the central Kuril Islands, *Nature*, *451*, 561–565, doi:10.1038/nature06521.
- Bautista, M. L. P., and K. Oike (2000), Estimation of the magnitudes and epicenters of Philippine historical earthquakes, *Tectonophysics*, *317*, 137–169, doi:10.1016/S0040-1951(99)00272-3.

- Bilek, S. L., S. Y. Schwartz, and H. R. DeShon (2003), Control of seafloor roughness on earthquake rupture behavior, *Geology*, *31*, 455–458, doi:10.1130/0091-7613(2003)031<0455:COSE>2.0.CO;2.
- Chapple, W. M., and D. W. Forsyth (1979), Earthquakes and bending of plates at trenches, *J. Geophys. Res.*, *84*(B12), 6729–6749, doi:10.1029/JB084iB12p06729.
- Christensen, D. H., and L. J. Ruff (1988), Seismic coupling and outer rise earthquakes, *J. Geophys. Res.*, *93*(B11), 13,421–13,444, doi:10.1029/JB093iB11p13421.
- Dmowska, R., J. R. Rice, L. C. Lovison, and D. Josell (1988), Stress transfer and seismic phenomena in coupled subduction zones during the earthquake cycle, *J. Geophys. Res.*, *93*(B7), 7869–7884, doi:10.1029/JB093iB07p07869.
- Kreemer, C., W. E. Holt, and A. J. Haines (2003), An integrated global model of present-day plate motions and plate boundary deformation, *Geophys. J. Int.*, *154*, 8–34, doi:10.1046/j.1365-246X.2003.01917.x.
- Lay, T., L. Astiz, H. Kanamori, and D. H. Christensen (1989), Temporal variation of large intraplate earthquakes in coupled subduction zones, *Phys. Earth Planet. Inter.*, *54*, 258–312, doi:10.1016/0031-9201(89)90247-1.
- Lay, T., H. Kanamori, C. J. Ammon, A. R. Hutko, K. Furlong, and L. Rivera (2009), The 2006–2007 Kuril Islands great earthquake sequence, *J. Geophys. Res.*, *114*, B11308, doi:10.1029/2008JB006280.
- Lay, T., C. J. Ammon, H. Kanamori, L. Rivera, K. D. Koper, and A. R. Hutko (2010), The 2009 Samoa–Tonga great earthquake triggered doublet, *Nature*, *466*, 964–968, doi:10.1038/nature09214.
- Lay, T., C. J. Ammon, H. Kanamori, M. J. Kim, and L. Xue (2011), Outer trench-slope faulting and the 2011 M_w 9.0 off the Pacific coast of Tohoku earthquake, *Earth Planets Space*, *63*, 713–718, doi:10.5047/eps.2011.05.006.
- Liu, X., and K. C. McNally (1993), Quantitative estimates of interplate coupling inferred from outer rise earthquakes, *Pure Appl. Geophys.*, *140*, 211–255, doi:10.1007/BF00879406.
- Nishenko, S. P. (1991), Circum-Pacific seismic potential—1989–1999, *Pure Appl. Geophys.*, *135*(2), 169–259, doi:10.1007/BF00880240.
- Raeesi, M., and K. Atakan (2009), On the deformation cycle of a strongly coupled plate interface: The triple earthquakes of 16 March 1963, 15 November 2006, and 13 January 2007 along the Kurile subduction zone, *J. Geophys. Res.*, *114*, B10301, doi:10.1029/2008JB006184.
- Rangin, C., X. Le Pichon, S. Mazzotti, M. Pubellier, N. Chamot-Rooke, M. Aurelio, A. Walpersdorf, and R. Quebral (1999), Plate convergence measured by GPS across the Sundaland/Philippine Sea Plate deformed boundary: The Philippines and eastern Indonesia, *Geophys. J. Int.*, *139*, 296–316, doi:10.1046/j.1365-246x.1999.00969.x.
- Song, T. A., and M. Simons (2003), Large trench-parallel gravity variations predict seismogenic behavior in subduction zones, *Science*, *301*(5633), 630–633, doi:10.1126/science.1085557.
- Taylor, M. A. J., G. Zheng, J. R. Rice, W. D. Stuart, and R. Dmowska (1996), Cyclic stressing and seismicity and strongly coupled subduction zones, *J. Geophys. Res.*, *101*(B4), 8363–8381, doi:10.1029/95JB03561.
- Toda, S., R. S. Stein, G. C. Beroza, and D. Marsan (2012), Aftershocks halted by static stress shadows, *Nat. Geosci.*, *5*, 410–413, doi:10.1038/ngeo1465.
- Todd, E. K., and T. Lay (2012), The 2011 Northern Kermadec Earthquake Doublet and subduction zone faulting interactions, *J. Geophys. Res.*, doi:10.1029/2012JB009711, in press.
- Venkataraman, A., and H. Kanamori (2004), Observational constraints on the fracture energy of subduction zone earthquakes, *J. Geophys. Res.*, *109*, B05302, doi:10.1029/2003JB002549.
- Yumul, G. P., Jr., C. B. Dimalanta, V. B. Maglambayan, and E. J. Marquez (2008), Tectonic setting of a composite terrane: A review of the Philippine island arc system, *Geosci. J.*, *12*, 7–17, doi:10.1007/s12303-008-0002-0.